Atmos. Chem. Phys. Discuss., 11, 14583–14605, 2011
www.atmos-chem-phys-discuss.net/11/14583/2011/
doi:10.5194/acpd-11-14583-2011

Atmospheric
Chemistry
and Physics
Discussions

Continental-scale enrichment of atmospheric $^{14}CO_2$ from the nuclear power industry: potential impact on the estimation of fossil fuel-derived CO_2

H. D. Graven[1,*] **and N. Gruber**[1]

[1] Institute of Biogeochemistry and Pollutant Dynamics, ETH Zurich, Universitätstrasse 16, 8092 Zurich, Switzerland
[*] now at: Scripps Institution of Oceanography, University of California-San Diego, 9500 Gilman Dr., La Jolla, CA 92093-0244, USA

Received: 26 April 2011 – Accepted: 27 April 2011 – Published: 12 May 2011

Correspondence to: H. D. Graven (hgraven@ucsd.edu)

Published by Copernicus Publications on behalf of the European Geosciences Union.

Abstract

Since aged carbon in fossil fuel contains no ^{14}C, ^{14}C/C ratios (Δ^{14}C) measured in atmospheric CO_2 can be used to estimate CO_2 added by combustion and, potentially, provide verification of fossil CO_2 emissions calculated using economic inventories. Sources of ^{14}C from nuclear power generation and spent fuel reprocessing can counteract dilution by fossil CO_2. Therefore, these nuclear sources can bias observation-based estimates of fossil fuel-derived CO_2 if they are not correctly accounted for or included as a source of uncertainty. We estimate annual ^{14}C emissions from each nuclear site in the world and conduct an Eulerian transport modeling study to investigate the continental-scale, steady-state gradients of Δ^{14}C caused by nuclear activities and fossil fuel combustion. Over Europe, North America and East Asia, nuclear enrichment may offset 0–260 % of the fossil fuel dilution in Δ^{14}C, corresponding to potential biases of 0 to −8 ppm in the CO_2 attributed to fossil fuel emissions, larger than the bias from respiration in some areas. Growth of ^{14}C emissions increased the potential nuclear bias over 1985–2005. The magnitude of this potential bias is largely independent of the choice of reference station in the context of Eulerian transport and inversion studies, but could potentially be reduced by an appropriate choice of reference station in the context of local-scale assessments.

1 Introduction

Since radiocarbon (^{14}C) is absent in highly aged fossil fuels, fossil fuel combustion strongly dilutes the ratio of ^{14}C/C in atmospheric CO_2, reported as Δ^{14}C including corrections for age and fractionation. Observations of Δ^{14}C allow dilution by ^{14}C-free fossil CO_2 to be quantified by comparison to Δ^{14}C observations at a clean air reference site (e.g., Levin et al., 2003) and may provide a means of validating CO_2 emissions calculated from economic data.

ACPD
11, 14583–14605, 2011

Atmospheric $^{14}CO_2$ gradients from nuclear industry

H. D. Graven and N. Gruber

Observation-based estimates of fossil fuel-derived CO_2 using $\Delta^{14}C$ can be biased, however, if other processes influencing $\Delta^{14}C$ are not correctly accounted for or considered as a source of uncertainty. Nuclear power and spent fuel reprocessing sites release ^{14}C in gaseous and liquid effluents, enriching ^{14}C of CO_2 in air and carbon in plant material and water surrounding nuclear sites by 4–20 000 ‰ (Levin et al., 1988, 2003; Dias et al., 2008). At the Heidelberg atmospheric sampling site in Germany, nuclear enrichment from a local reactor has been corrected for using dispersion modeling of observed ^{14}C emissions at that reactor (Levin et al., 2003).

Nuclear ^{14}C emissions may also contribute to $\Delta^{14}C$ gradients at larger, i.e. continental, scales since a high-emission site or a high density of sites may cause $\Delta^{14}C$ enrichment that expands well beyond the local to regional scale, corresponding to areas of 1 to 10 000 km^2. The potential for such continental-scale gradients of $\Delta^{14}C$ in CO_2 has not yet been explored. A previous modeling study found that the $\Delta^{14}C$ enrichment caused by the nuclear industry was negligible, but this study unrealistically applied ^{14}C emissions homogeneously across northern continental regions without considering the spatial distribution of individual nuclear sites (Turnbull et al., 2009). We will show that accurately representing the location and magnitude of nuclear sources in transport model simulations causes substantial continental-scale $\Delta^{14}C$ gradients that significantly counteract gradients caused by fossil fuel emissions in some places.

In order to investigate the potential for ^{14}C emissions from the nuclear energy industry to cause continental-scale gradients in $\Delta^{14}C$, we estimate ^{14}C emissions from individual nuclear sites and conduct Eulerian atmospheric transport simulations of spatially-resolved nuclear $^{14}CO_2$ and fossil fuel CO_2 sources. We assess the potential for $\Delta^{14}C$ gradients from nuclear ^{14}C emissions to cause biases in fossil fuel CO_2 at continental scales and compare the pattern and magnitude of the potential nuclear biases to those arising from ^{14}C exchange with the ocean and terrestrial biosphere (Turnbull et al., 2009). By compiling observed ^{14}C emission rates, we also consider variability and uncertainty in nuclear ^{14}C emissions.

Unlike previous work examining the dispersion of temporary, severe radioactive sources using Lagrangian approaches (e.g., Klug et al., 1992; Draxler and Hess, 1998), our study focuses on ^{14}C emissions from multiple nuclear sites that occur continually within continental regions of the Northern Hemisphere. These ^{14}C emissions are part of the normal operating procedures of the nuclear sites and are within government-imposed limits. We use an Eulerian framework, rather than a Lagrangian framework, to estimate steady-state gradients over large scales. This Eulerian framework is similar to that used in global and regional inversions of CO_2 that exploit gradients between observation stations located 100–10 000 km from one another (e.g., Gurney et al., 2002), as well as in other studies of continental Δ^{14}C gradients (Hsueh et al., 2007; Turnbull et al., 2009). Our results therefore have specific relevance for applications utilizing observed Δ^{14}C gradients at these scales, while they do not address the small-scale gradients that exist in the local vicinity of individual nuclear sites and may also influence Δ^{14}C at some observation sites.

2 Methods

2.1 $^{14}CO_2$ emissions from individual nuclear power plant sites

Radiocarbon is produced mainly through reactions of nitrogen impurities and oxygen in uranium oxide fuel or coolant water of nuclear reactors, but also in structural material, in the graphite of graphite-moderated reactors and the cooling gas of gas-cooled reactors (Yim and Caron, 2006). Nearly all ^{14}C is released in the form of $^{14}CO_2$, except in Pressurized Water Reactors (PWRs) where ^{14}C is mainly released as $^{14}CH_4$ (Kunz, 1985; Uchrin et al., 1998; Van der Stricht and Janssens, 2001, 2005). We assume the lifetime of $^{14}CH_4$ (approx. 10 yr; Prather, 1994) to be too long to contribute to continental-scale gradients in Δ^{14}C of CO_2, permitting us to neglect $^{14}CH_4$ emissions.

Only 20–25 % of all nuclear sites measure and report ^{14}C emissions (Fig. 1), so we use ^{14}C emission factors, i.e. the ratio of ^{14}C emissions over electrical energy output, to estimate ^{14}C emissions at all sites. Annual energy output for each reactor in operation between 1985 and 2005 was compiled from the International Atomic Energy Agency's Power Reactor Information System (IAEA PRIS, available at http://www.iaea.org/programmes/a2/index.html). We use $^{14}CO_2$ emission factors of: 0.06 TBq GWa^{-1} for PWRs, 0.51 TBq GWa^{-1} for Boiling Water Reactors (BWRs), 1.6 TBq GWa^{-1} for Heavy Water Reactors (HWRs), 1.4 TBq GWa^{-1} for Advanced Gas-Cooled Reactors (GCRs), 5.5 TBq GWa^{-1} for Magnox GCRs, 1.3 TBq GWa^{-1} for Light-Water-cooled Graphite-moderated Reactors (LWGRs) and 0.12 TBq GWa^{-1} for Fast Breeder Reactors (FBRs). These emission factors were given as averages for 1990–1995 in UNSCEAR (2000). We reduced the emission factor for PWRs by 75 % to account for ^{14}C released as methane (Kunz, 1985; Uchrin et al., 1998; Van der Stricht and Janssens, 2001, 2005) and increased the emission factor for Magnox-type GCRs by a factor of 4 based on observed emission rates (Fig. 1, UKEA 1996–2008). Estimated emissions of ^{14}C from each nuclear site are tabulated in the auxiliary material.

Total electrical energy output by all nuclear reactors nearly doubled between 1985 and 2005, while total ^{14}C emissions (including $^{14}CH_4$) increased by only 40–60 %, from 89 [43, 172] to 130 [69, 280] TBq yr^{-1} (bracketed values indicate 70 % confidence intervals). This is because most of the growth in electrical output was generated by PWR- and BWR-type reactors that release comparatively less ^{14}C. Total ^{14}C release represented about 10 % of the average production rate from cosmogenic radiation (Masarik and Beer, 1999).

The ^{14}C emission factors are associated with substantial uncertainties as they vary, for example, due to episodic venting, replacement of resin columns and other maintenance (Kunz, 1985; Stenström et al., 1995; Sohn et al., 2004). To examine temporal and site-to-site variability, we compiled available observations of gaseous ^{14}C emissions and compared them to electrical energy output at several individual PWRs, BWRs, HWRs and GCRs (Fig. 1). Observations at LWGRs (Konstantinov et al., 1989) were consistent with UNSCEAR (2000). No observations from FBRs were found.

Substantial variability spanning 300–1000 % was found in the observations for different reactors and for individual reactors over several years, particularly in PWRs, HWRs and Magnox GCRs. No consistent differences between reactors in different countries were apparent. We calculated the 15 and 85 % limits of the lognormal cumulative distribution of the observations for each reactor type in Fig. 1 to define a 70 % confidence interval for the emission factors, similar to a 1-sigma uncertainty in a normal distribution. We apply the observed confidence intervals to estimate uncertainty in ^{14}C emissions and uncertainty in the resulting enrichment in atmospheric $^{14}CO_2$ (Sects. 3 and 4).

Theoretical estimates of ^{14}C emission factors (Fig. 1; Yim and Caron, 2006) were similar to observations for PWR and BWRs, but quite different for HWRs and GCRs. This is likely a result of theoretical estimates not accounting for ^{14}C capture at some HWRs and GCRs or the poorly-known release of ^{14}C produced in the moderators of GCRs.

2.2 ^{14}C emissions from other sources

Dissolution of spent nuclear fuel during reprocessing liberates ^{14}C, which is released in gaseous effluents as $^{14}CO_2$ (Koarashi et al., 2005). We compiled observations of ^{14}C released between 1985 and 2005 at 3 active spent fuel reprocessing sites where ^{14}C is released: La Hague, France, Sellafield, UK and Tokai, Japan (UNSCEAR, 1988, 1993, 2000; Schneider and Marignac, 2008; Nakada et al., 2008; UKEA, 1996–2008), also tabulated in the auxiliary material. Total ^{14}C release from spent fuel reprocessing from these 3 sites over 1985–2005 was roughly 10 % of the release from nuclear power generation.

Our estimates of total ^{14}C emissions do not include some additional anthropogenic ^{14}C sources, despite the fact that they could also contribute to ^{14}C enrichment at continental scales. These sources include emissions from experimental research reactors, reactors that were recently shutdown, radiochemical production facilities, military operations, and disposal or incineration sites for medical or research waste. We omitted these sources due to lack of data on emission rates and chemical forms of ^{14}C. However, observations from research reactors in Germany (BMU, 2002–2008) and a radiochemical production facility in the UK (UKEA, 1996–2008) showed ^{14}C emissions that were similar to medium- to large-sized BWRs. Emissions from newly shutdown reactors can be as large as 300 % of the average release during active periods (BMU, 2002–2008; UKEA, 1996–2008), but are neglected here by our use of emission factors that are tied to electrical production. As a result, our estimated ^{14}C emission from the nuclear power industry does not comprise the total anthropogenic emission of ^{14}C.

2.3 Transport modeling

Surface fluxes of ^{14}C from nuclear sites and CO_2 from fossil fuel combustion were used as boundary conditions in simulations of the global TM3 atmospheric transport model with 1.8° × 1.8° resolution and 28 vertical levels (Heimann and Korner, 2003). Annual mean emissions of CO_2 from fossil fuel combustion were given by the Emissions Database for Global Atmospheric Research version 4.0 (EDGAR, available at http://edgar.jrc.ec.europa.eu/index.php) for individual years 1985–2005, aggregated from 0.1° to 1.8° resolution.

We computed 4-yr simulations with constant fluxes corresponding to each year 1985–2005, similar to the specifications of the Transcom 3 Experiment (Gurney et al., 2000), and averaged the simulated concentrations over the 4th year. Meteorological forcing was given by 6-h NCEP reanalysis fields specific to each year 1985–2005 (Kalnay et al., 1996).

We examine gradients in Δ^{14}C over three continental regions in the Northern Hemisphere, relative to a regional reference site: Niwot Ridge, USA (NWR, 3.75 km a.s.l.) for North America, Jungfraujoch, Switzerland (JFJ, 3.45 km a.s.l.) for Europe and Mt. Waliguan, China (WLG, 3.81 km a.s.l.) for Asia (Fig. 2a–c). Spatial maps of gradients in Δ^{14}C in the lowest model level are presented for 2005 in Sect. 3, while temporal changes at selected sites are presented in Sect. 4.

Gradients were calculated using the simulated enhancement in CO_2 (δC_{ff}) or $^{14}CO_2$ (δA_{nuc}) relative to the regional reference sites, i.e. $\delta C_{\mathrm{ff}} = \overline{C_{\mathrm{ff}}} - \overline{C^R_{\mathrm{ff}}}$ and $\delta A_{\mathrm{nuc}} = \overline{A_{\mathrm{nuc}}} - \overline{A^R_{\mathrm{nuc}}}$, where R indicates the reference site. The dilution in $\Delta^{14}C$ caused by fossil fuel emissions, $\delta\Delta_{\mathrm{ff}}$, and the enhancement in $\Delta^{14}C$ caused by nuclear emissions, $\delta\Delta_{\mathrm{nuc}}$, were calculated by:

$$\delta\Delta_{\mathrm{ff}} = -\delta C_{\mathrm{ff}} \frac{1000\,\text{‰} + \Delta_R}{C_R + \delta C_{\mathrm{ff}}} \tag{1}$$

$$\delta\Delta_{\mathrm{nuc}} = \frac{\delta A_{\mathrm{nuc}} 1000\,\text{‰}}{R_{\mathrm{s}}(C_R + \delta C_{\mathrm{ff}})} \tag{2}$$

These equations were derived by approximate mass balance of carbon and ^{14}C. R_{s} is 1.176×10^{-12}, the $^{14}C/C$ ratio in the Modern Standard. The change in $\Delta^{14}C$ also depends on the background air CO_2 mixing ratio and $\Delta^{14}C$ (C_R and Δ_R), which was assigned to be the global average for each year (Table S1). We use global average values at each regional reference site since observations are not available for all sites in all years. Though annual mean $\Delta^{14}C$ and CO_2 in Northern Hemisphere background air can vary by ± 5 ‰ and ± 1.6 ppm from the estimated global average (Levin et al., 2010; Graven et al., 2011; Keeling and Whorf, 2005), the potential error in $\delta\Delta_{\mathrm{ff}}$ caused by using global average values at the regional reference sites is less than 0.8 %.

Since the spatial gradients in fossil fuel CO_2 are small relative to the absolute concentration of CO_2 in the atmosphere, i.e., $\delta C_{\mathrm{ff}} \ll C_R$, the dilution of $\Delta^{14}C$ by fossil fuel emissions ($\delta\Delta_{\mathrm{ff}}$) relates to δC_{ff} by a roughly constant factor of -2.8 ‰ : 1 ppm in 2005. The bias in δC_{ff} that would occur if nuclear ^{14}C enrichment was not accounted for (β_{nuc}) similarly relates to $\delta\Delta_{\mathrm{nuc}}$ by approximately -2.8 ‰ : 1 ppm, since nuclear enrichment reduces apparent $\delta\Delta_{\mathrm{ff}}$.

We performed sensitivity tests to evaluate the effect of uncertainty in ^{14}C emission factors and the choice of regional reference site. To test the effect of uncertainty in the emission factors, we performed additional simulations for emissions calculated with emission factors at the lower and upper limits of the 70 % confidence intervals shown in Fig. 1. To test the sensitivity to the choice of reference site, we additionally calculated Δ^{14}C gradients relative to free tropospheric air at 2.9 km a.s.l. (the 10th model level).

3 Regional gradients in Δ^{14}C of CO_2

The largest simulated δC_{ff} of 11–18 ppm was associated with the most densely populated areas (Fig. 2a–c), while over large regions of North America, Europe, and Asia δC_{ff} exceeded 0.5 ppm ($\delta\Delta^{14}\mathrm{C} < -1.4$ ‰). In contrast, nuclear ^{14}C emissions enhanced Δ^{14}C by more than 0.7 ‰ over large regions of North America, Europe and Asia in 2005 (Fig. 2d–f), offsetting the dilution of Δ^{14}C from fossil fuel emissions substantially.

The largest $\delta\Delta_{\mathrm{nuc}}$ (22 ‰) and β_{nuc} (–8 ppm) was simulated over northern France and the UK due to releases from La Hague and Sellafield reprocessing sites and several Gas-Cooled Reactors. Though enhancement of Δ^{14}C was largest in grid cells containing large nuclear sources, negative values of β_{nuc} extend far into downwind regions without nuclear sources. Outflow from northern France and the UK contributed to high $\delta\Delta_{\mathrm{nuc}}$ and β_{nuc} over much of Northern Europe (Fig. 2e). The Great Lakes region of North America, central Japan and South Korea also showed substantial $\delta\Delta_{\mathrm{nuc}}$ and β_{nuc} extending > 400 km away from nuclear sites.

The relative magnitude of the potential biases in inferred fossil fuel-derived CO_2, i.e. the absolute of the ratio of β_{nuc} to δC_{ff}, can amount to more than 100 % (Fig. 2g–i). Over the English Channel, β_{nuc} was as large as 260 % of δC_{ff}. In large regions, such as Eastern Canada, Northwestern France, the UK, Ireland, the Baltic Sea, Russia and Japan, the potential bias remained above 20 %. There were also areas with very little potential bias, owing to intense fossil fuel emissions but little to no nuclear activity, such as over the west coast of North America and most of China.

Simulated β_{nuc} for 2005 using emission factors at the 15 % and 85 % limits of the cumulative distribution of observed emission factors are shown in Fig. 3. Increasing emission factors to the upper limit caused β_{nuc} to be 300 % larger, on average. The area of $\beta_{nuc} < -0.25$ ppm spread over the Atlantic Ocean, Eastern Canada, Russia, Scandinavia, Southern Europe, China and Korea. In these areas, β_{nuc} was generally larger than 20 % of δC_{ff}. In simulations with emission factors at the lower limit, $\delta\Delta_{nuc}$ and β_{nuc} became 60 % smaller in North America and Asia and 40 % smaller in Europe, on average. Potential biases were much less important in North America and Asia, but in large regions of Northern Europe β_{nuc} was still comparable in magnitude to δC_{ff} (> 20 %). Patterns were largely the same when we used free tropospheric air as the background instead of the continental reference sites, and δC_{ff} changed by less than ±0.1 ppm and β_{nuc} changed by less than ±0.01 ppm in more than 85 % of grid cells shown in Fig. 2g–i.

4 Temporal changes in δC_{ff} and β_{nuc}

Concurrent changes to the patterns and magnitudes of fossil fuel and nuclear emissions could cause spurious trends in δC_{ff} inferred from $\Delta^{14}C$ observations. To estimate the potential for such an effect, we examine modeled annual mean δC_{ff} and β_{nuc}, relative to the continental reference sites, over 1985–2005 at 6 sites where $\Delta^{14}C$ in CO_2 is currently measured or may be initiated in the future: Cape May, USA (CMA) and Sable Island, Canada (SBL) in North America; Lutjewad, Netherlands (LUT) and Schauinsland, Germany (SCH) in Europe; and Gosan, South Korea (GSN) and Ryori, Japan (RYO) in Asia.

Modeled δC_{ff} was between 1 and 7 ppm at the 6 sites over 1985–2005 (Fig. 4a–c). At each site, δC_{ff} spanned ±0.2 to ±1.0 ppm from the mean value due to an overall trend and/or to variations in emission and atmospheric transport. β_{nuc} was −0.1 to −0.8 ppm, with the largest negative potential biases at Cape May, Lutjewad and Ryori (Fig. 4d–f).

At all sites, β_{nuc} grew in proportion to δC_{ff} (Fig. 4g–i) as the number and activity of nuclear reactors expanded between 1985–2005 and, at the European sites, as δC_{ff} decreased. A strong increase in β_{nuc} is apparent at Gosan, caused by the implementation of 3 Heavy Water Reactors at Wolsong, South Korea in the 1990s. To assess the impact of growth in β_{nuc} on the apparent trend in δC_{ff}, we compare 5-yr means of δC_{ff} and $\delta C_{ff} + \beta_{nuc}$ for 1985–1989 and 2001–2005 (Table 1). Simulated δC_{ff} increased at the North American and Asian sites and decreased at the European sites between 1985–1989 and 2001–2005. Including the simultaneous change in β_{nuc} caused δC_{ff} to appear to have increased 6–7 % less at Cape May and Gosan, to have decreased 2–3 % more at Schauinsland and Lutjewad, and to have decreased by 4–5 % instead of increased by 1–2 % at Sable Island and Ryori. The largest effects were at Cape May and Ryori, significantly larger in magnitude than uncertainties in the fractional change in local δC_{ff} or $\delta C_{ff} + \beta_{nuc}$ due to variations in emission and atmospheric transport. Our results indicate that concurrent trends in β_{nuc} can bias and change the sign of Δ^{14}C-based observations of δC_{ff} trends.

δC_{ff} calculated in comparison to free tropospheric air was 3–40 % smaller than δC_{ff} calculated using the continental reference sites, except at Schauinsland where it was slightly larger. However, in comparison to free tropospheric air, β_{nuc} was simultaneously reduced by a comparable amount (1–44 %) so that the ratio of β_{nuc} to δC_{ff} changed very little.

Simulations using emission factors at the limits of 70 % confidence demonstrate very large uncertainties that are skewed toward stronger β_{nuc} (Fig. 4). At the upper limit, β_{nuc} compensated 15–50 % of the dilution from δC_{ff} at the sites. At the lower limit, β_{nuc} compensated 5–10 % of δC_{ff}. These uncertainties further complicate the identification of trends in δC_{ff} using Δ^{14}C observations. While we have set emission factors to either the lower or upper limit at all sites, the observations show that emission factors at each site vary from year to year (Fig. 1), which may cause different patterns and larger variability than our simulations.

5 Discussion and conclusions

Our simulation of ^{14}C emissions from individual nuclear sites in the Northern Hemisphere shows that these ^{14}C emissions contribute to a Δ^{14}C enrichment at continental scales that is substantial enough to partially counteract the fossil fuel dilution effect. The potential nuclear bias to δC_{ff} can extend over spatial scales on the order of 1000 km and can be as large as −8 [−7, −16] ppm. Our simulated β_{nuc} at Cape May, −0.8 [−0.3, −1.8] ppm for 2005, is substantially larger than Turnbull et al. (2009), who simulated β_{nuc} of only 0 to −0.2 ppm over 2002–2008. This is a consequence of us emitting the nuclear ^{14}C from point sources rather than spreading the emissions homogenously over the northern continents as in Turnbull et al. (2009). Accounting for the spatial distribution of nuclear sites reveals several regions with a high density of ^{14}C sources, particularly Northern France and the UK and the Eastern US and Canada, that are important to consider in accurately determining continental-scale gradients.

The broad spatial patterns we simulated using an Eulerian transport modeling approach are particularly evident, for example, in the ^{14}C outflow to Northern Europe from reprocessing sites and Gas-Cooled Reactors in Northern France and the UK. These continental-scale gradients are caused by the aggregate influence on Δ^{14}C from all nuclear sites in the region, which cannot be accounted for by dispersion modeling of nearby reactors only. Comparison of observed Δ^{14}C to a reference site > 100–200 km away may therefore include a substantial continental-scale effect, in addition to any local-scale effects from nearby reactors. Observational studies at finer (urban) scales may be effective in reducing the continental-scale β_{nuc} by using local observation sites to define background air composition, particularly in areas that are far from nuclear sources.

While our objective was not to resolve local-scale dispersion and transport, simulated continental-scale β_{nuc} is still highly dependent on model resolution such that stronger gradients exist within the 100–200 km grid used in the rather coarse TM3 simulations. Higher resolution regional models are likely to provide better estimates of continental-scale β_{nuc} at particular sites. Higher resolution models may also represent transport to high altitude sites more accurately. Our results are also sensitive to errors in model transport, particularly in the vertical transport out of the boundary layer, though TM3 shows realistic vertical profiles of CO_2 on an annual mean basis (Stephens et al., 2007).

The potential bias in δC_{ff} caused by nuclear ^{14}C releases may be as large or larger than the potential bias caused by respiration of ^{14}C-enriched carbon from terrestrial ecosystems over some areas. Turnbull et al. (2009) simulated biases caused by respiration in recent years to be −0.2 ppm above northern continents on average, and as large as −1 ppm, consistent with model results of $\Delta^{14}C$ enrichment of 0–2 ‰ above North America by Hsueh et al. (2007). Our results show potential biases of 0 to −8 [−7, −16] ppm, with stronger gradients in β_{nuc} than those resulting from relatively homogeneous biospheric sources. Together, nuclear and respiratory influences on $\Delta^{14}C$ likely cause potential negative biases in δC_{ff} larger than 0.5 ppm over large regions of the Northern Hemisphere. Continental gradients of $\Delta^{14}C$ caused by air-sea exchange are much smaller than nuclear and biospheric influences in the Northern Hemisphere (Hsueh et al., 2007; Turnbull et al., 2009).

Measurement precision in $\Delta^{14}C$ of atmospheric CO_2 currently limits detection to $\delta C_{ff} > 0.5$ ppm, while the specification of background air composition adds further uncertainty of ±0.5–1.9 ppm (Turnbull et al., 2009; Graven et al., 2009). Our simulations suggest that the magnitude of β_{nuc} is likely to exceed total observational uncertainty in δC_{ff} over Eastern North America, Northwestern Europe and parts of Japan and Korea (Fig. 2d–f).

Estimates of ^{14}C emissions include substantial uncertainties. The observed variability in emission factors (Fig. 1) suggests that β_{nuc} could be much stronger (+300 %) or weaker (−60 %) in magnitude than illustrated in Fig. 2. Moreover, ^{14}C emissions can vary strongly between different reactors or years (Fig. 1; Sect. 2.1) and can occur in discrete periods when the reactor effluent is vented to the atmosphere.

In the coming decades, nuclear ^{14}C release may become more important; 58 nuclear power reactors are currently under construction, with the largest share (23) in China. Nearly all the reactors will be of the Pressurized Water Reactor type that has the lowest emission factor. However, a high density of low-^{14}C release reactors caused biases up to −1.5 ppm in Germany (Fig. 2e). At the same time, some older high-^{14}C release reactors, including Magnox-type gas-cooled reactors in the UK, are being shut down. Whether ^{14}C releases grow or decline, trends in β_{nuc} can bias the apparent change in δC_{ff} over time and complicate the use of atmospheric Δ^{14}C to identify growth or reduction in CO_2 emissions. Trends in β_{nuc} caused potential biases of 2–7 % in δC_{ff} trends in our simulations, comparable to the emissions reductions agreed upon in the Kyoto Protocol.

Our results suggest that the influence of nuclear activities on atmospheric Δ^{14}C must be correctly accounted for in large regions of North America, Europe and Asia to estimate δC_{ff} accurately using observations of Δ^{14}C in CO_2. High resolution ^{14}C release data from each nuclear reactor site would improve estimates of Δ^{14}C enrichment by transport modeling. Alternatively, measures to reduce or eliminate ^{14}C release would improve accuracy in observation-based estimates of δC_{ff}, though such measures would cause temporal changes to β_{nuc} that would influence apparent trends in δC_{ff}.

Supplementary material related to this article is available online at: http://www.atmos-chem-phys-discuss.net/11/14583/2011/ acpd-11-14583-2011-supplement.zip.

Acknowledgements. We thank C. Rödenbeck for assistance with the TM3 model and M.-S. Yim and F. Caron for helpful discussions. This work was financially supported by ETH Zurich.

References

BMU: Umweltradioaktivität und Strahlenbelastung, Tech. rep., Bundesumweltministerium, Bonn, Germany, 2002–2008. 14589

Dias, C., Santos, R., Stenström, K., Nícoli, I., Skog, G., and da Silveira Corrêa, R.: ^{14}C content in vegetation in the vicinities of Brazilian nuclear power reactors, J. Environ. Rad., 99(7), 1095–1101, 2008. 14585

Draxler, R. R. and Hess, G. D.: An overview of the HYSPLIT_4 modelling system for trajectories, dispersion, and deposition, Austral. Meteorol. Mag., 47(4), 295–308, 1998. 14586

Graven, H. D., Stephens, B. B., Guilderson, T. P., Campos, T. L., Schimel, D. S., Campbell, J. E. and Keeling, R. F.: Vertical profiles of biospheric and fossil fuel-derived CO_2 and fossil fuel CO_2 : CO ratios from airborne measurements of Δ^{14}C, CO_2 and CO above Colorado, USA, Tellus B, 61, 536–546, 2009. 14595

Graven, H. D., Guilderson, T. P., and Keeling, R. F.: Observations of radiocarbon in CO_2 at La Jolla, California, USA 1992–2007, J. Geophys. Res., submitted, 2011. 14590

Gurney, K., Law, R., and Rayner, P.: Transcom 3 experimental protocol, Department of Atmospheric Science, Colorado State University, Fort Collins, Colorado, USA, Paper 707, 2000. 14589

Gurney, K. R., Law, R. M., Denning, A. S., Rayner, P. J., Baker, D., Bousquet, P., Bruhwiler, L., Chen, Y.-H., Ciais, P., Fan, S., Fung, I. Y., Gloor, M., Heimann, M., Higuchi, K., John, J., Maki, T., Maksyutov, S., Masarie, K., Peylin, P., Prather, M., Pak, B. C., Randerson, J., Sarmiento, J., Taguchi, S., Takahashi, T., and Yuen, C.-W.: Towards robust regional estimates of CO_2 sources and sinks using atmospheric transport models, Nature, 415, 626–630, 2002. 14586

Heimann, M., and Korner, S.: The Global Atmospheric Tracer Model TM3, Model Description and Users Manual Release 3.8a, Technical Report 5, Max Planck Institute for Biogeochemistry (MPIBGC), Jena, Germany. 14589

Hsueh, D. Y., Krakauer, N. Y., Randerson, J. T., Xu, X., Trumbore, S. E., and Southon, J. R.: Regional patterns of radiocarbon and fossil fuel-derived CO_2 in surface air across North America, Geophys. Res. Lett., 34, L02816, doi:10.1029/2006GL027032, 2007. 14586, 14595

Kalnay, E., Kanamitsu, M., Kistler, R., Collins, W., Deaven, D., Gandin, L., Iredell, M., Saha, S., White, G., Woollen, J., Zhu, Y., Leetmaa, A., Reynolds, R., Chelliah, M., Ebisuzaki, W., Higgins, W., Janowiak, J., Mo, K. C., Ropelewski, C., Wang, J., Jenne, R., and Joseph, D.: The NCEP/NCAR 40-Year Reanalysis Project, B. Am. Meteorol. Soc., 77(3), 437–472, 1996.

14589

Keeling, C. D. and Whorf, T. P.: Atmospheric CO_2 records from sites in the SIO air sampling network, in: Trends: a Compendium of Data on Global Change, Carbon Dioxide Information Analysis Center, Oak Ridge National Laboratory, US Department of Energy, Oak Ridge, TN, 2005. 14590

Klug, W., Graziani, G., Grippa, G., Pierce, D., and Tassone, C.: Evaluation of long range atmospheric transport models using environmental activity data from the Chernobyl accident (The ATMES Report), Elsevier Applied Science, London and New York, 1992. 14586

Koarashi, J., Akiyama, K., Asano, T., and Kobayashi, H.: Chemical composition of ^{14}C in airborne release from the Tokai reprocessing plant, Japan, Rad. Prot. Dosimetry, 114(4), 551–555, 2005. 14588

Konstantinov, E. A., Korablev, N. A., Solov'ev, E. N., Shamov, V. P., Fedorov, V. L., and Litvinov, A. M.: ^{14}C emission from RBMK-1500 reactors and features determining it, Atomic Energy, 66(1), 77–79, 1989. 14587

Kunz, C.: Carbon-14 discharge at three light-water reactors, Health Phys., 49(1), 25–35, 1985. 14586, 14587

Levin, I., Kromer, B., Barabas, M., and Muennich, K. O.: Environmental distribution and long-term dispersion of reactor $^{14}CO_2$ around two German nuclear power plants, Health Phys., 54(2), 149–156, 1988. 14585

Levin, I., Kromer, B., Schmidt, M., and Sartorius, H.: A novel approach for independent budgeting of fossil fuel CO_2 over Europe by $^{14}CO_2$ observations, Geophys. Res. Lett., 30(23), 2194, doi:10.1029/2003GL018477, 2003. 14584, 14585

Levin, I., Naegler, T., Kromer, B., Diehl, M., Francey, R. J., Gomez-Pelaez, A. J., Steele, L. P., Wagenbach, D., Weller, R., and Worthy, D. E.: Observations and modelling of the global distribution and long-term trend of atmospheric $^{14}CO_2$, Tellus B, 62, 26–46, 2010. 14590

Masarik, J., and Beer, J.: Simulation of particle fluxes and cosmogenic nuclide production in the Earth's atmosphere, J. Geophys. Res., 104(D10), 12099–12112, 1999. 14587

Nakada, A., Miyauchi, T., Akiyama, K., Momose, T., Kozawa, T., Yokota, T., and Ohtomo, H.: Radioactive Airborne Effluent Discharged from Tokai Reprocessing Plant (1998–2007), Tech. rep., Japan Atomic Energy Agency, Tokai-mura, Japan, 2008. 14588

Prather, M. J.: Lifetimes and eigenstates in atmospheric chemistry, Geophys. Res. Lett., 21(9), 801–804, 1994. 14586

Schneider, M. and Marignac, Y.: Spent Nuclear Fuel Reprocessing in France, Research Report

4, International Panel on Fissile Materials, Princeton, New Jersey, USA, 2008. 14588

Sohn, W., Kang, D. W., and Chi, J.: Approaches for reducing carbon-14 stack emissions from Korean CANDU® nuclear power plant, J. Nucl. Sci. Technol., 41(2), 235–246, 2004. 14587

Stenström, K., Erlandsson, B., Hellborg, R., Wiebert, A., Skog, S., Vesanen, R., Alpsten, M., and Bjurman, B.: A one-year study of the total air-borne ^{14}C effluents from two Swedish light-water reactors, one boiling water and one pressurized water reactor, J. Radioanal. Nucl. Chem., 198(1), 203–213, 1995. 14587

Stephens, B. B., Gurney, K. R., Tans, P. P., Sweeney, C., Peters, W., Bruhwiler, L., Ciais, P., Ramonet, M., Bousquet, P., Nakazawa, T., Aoki, S., Machida, T., Inoue, G., Vinnichenko, N., Lloyd, J., Jordan, A., Heimann, M., Shibistova, O., Langenfelds, R. L., Steele, L. P., Francey, R. J., and Denning, A. S.: Weak northern and strong tropical land carbon uptake from vertical profiles of atmospheric CO_2, Science, 316(5832), 1732, 2007. 14595

Turnbull, J., Rayner, P., Miller, J. B., Naegler, T., Ciais, P., and Cozic, A.: On the use of $^{14}CO_2$ as a tracer for fossil fuel CO_2: quantifying uncertainties using an atmospheric transport model, J. Geophys. Res., 114, D22302, doi:10.1029/2009JD012308, 2009. 14585, 14586, 14594, 14595

Uchrin, G., Hertelendi, E., Volent, G., Slávik, O., Morávek, J., Kobal, I., and Vokal, B.: ^{14}C measurements at PWR-type nuclear power plants in three middle European countries, Radiocarbon, 40, 439–446, 1998. 14586, 14587

UKEA: Radioactivity in Food and the Environment, UK Environment Agency, 1996–2008. 14587, 14588, 14589

UNSCEAR: Sources and effects of ionizing radiation, Report of the United Nations Scientific Committee on the Effects of Atomic Radation, Vienna, 1988, 1993 and 2000. 14587, 14588

Van der Stricht, S. and Janssens, A.: Radioactive effluents from nuclear power stations and nuclear fuel reprocessing sites in the European Union, Radiation Protection, European Commission, 2001 and 2005. 14586, 14587

Yim, M. S. and Caron, F.: Life cycle and management of carbon-14 from nuclear power generation, Progress Nucl. Energy, 48(1), 2–36, 2006. 14586, 14588, 14602

Table 1. Change in simulated δC_{ff} and $\delta C_{ff} + \beta_{nuc}$ between 5-yr means for 1985–89 and 2001–05 at the sites shown in Fig. 4. Uncertainties were calculated using the standard error in simulated δC_{ff} and $\delta C_{ff} + \beta_{nuc}$ over the 5-yr periods, which comprise only variations in emissions and atmospheric transport over the 5-yr periods. Uncertainties in ^{14}C emission factors are not included.

	$\Delta\delta C_{ff}$ (%)	$\Delta(\delta C_{ff} + \beta_{nuc})$ (%)	difference (%)
CMA	$+26 \pm 4$	$+19 \pm 3$	−7
SAB	$+1 \pm 6$	-4 ± 6	−5
SCH	-5 ± 5	-8 ± 5	−3
LTW	-8 ± 5	-10 ± 6	−2
RYO	$+2 \pm 4$	-5 ± 5	−7
GSN	$+38 \pm 9$	$+32 \pm 7$	−6

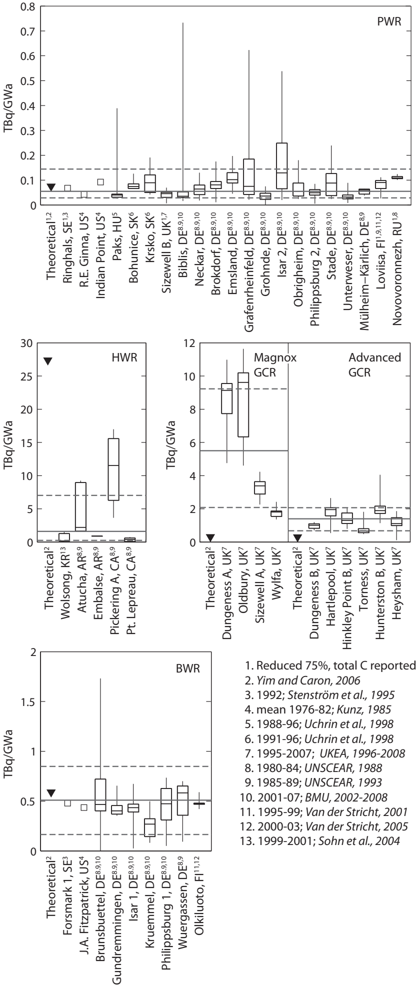

Fig. 1. Caption on next page.

Fig. 1. Emission factors of $^{14}CO_2$ release per electrical energy output at nuclear reactors of Pressurized Water Reactor (PWR), Heavy Water Reactor (HWR), Magnox and Advanced Gas-Cooled Reactor (GCR) and Boiling Water Reactor (BWR) types. Triangles indicate theoretical emission factors from Yim and Caron (2006). Observed emission factors at individual nuclear sites are shown as squares when one year or one multi-year average observation of $^{14}CO_2$ release was reported, or as boxplots when several years of annual mean observations were reported. Dashed lines show 70 % confidence intervals. Emission factors at PWRs footnoted with a "1" reported total ^{14}C release and were reduced by 75 % to account for $^{14}CH_4$ emissions. Other footnotes indicate the periods of observation and references. Solid lines show emission factors used, as listed in Sect. 2.1.

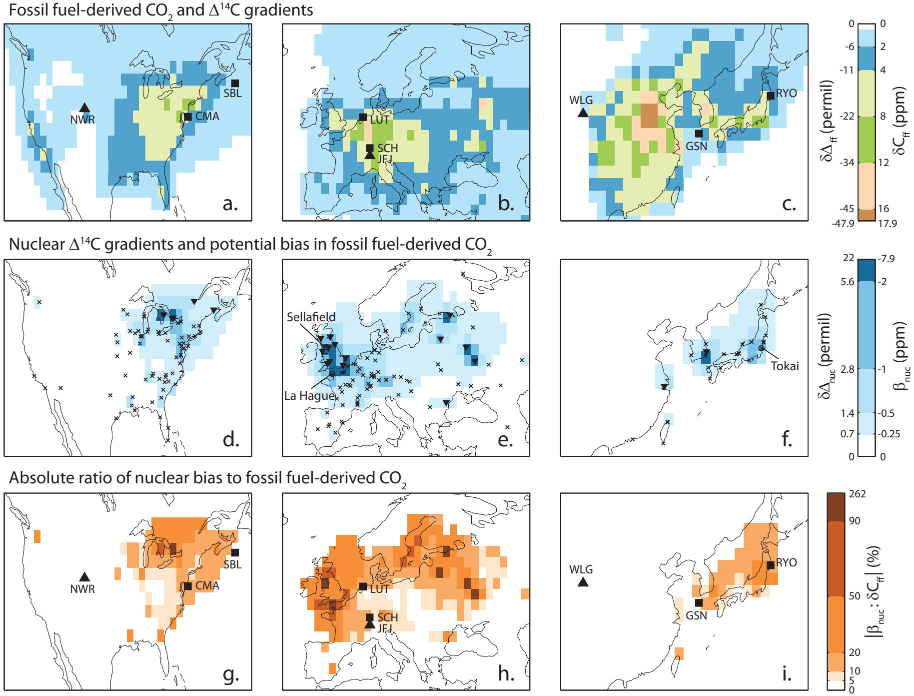

Fig. 2. (a–c) Maps of fossil fuel-derived CO_2 (δC_{ff}) and $\Delta^{14}C$ dilution ($\delta\Delta_{ff}$) in continental regions of the Northern Hemisphere. Regional reference sites are indicated by triangles and observation sites by squares. **(d–f)** Nuclear $\Delta^{14}C$ enhancement ($\delta\Delta_{nuc}$) and potential nuclear bias to fossil fuel-derived CO_2 (β_{nuc}). Locations of low-^{14}C release reactors are indicated by crosses, high-^{14}C release reactors by triangles, and spent fuel reprocessing sites are labeled. **(g–i)** The ratio $|\beta_{nuc} : \delta C_{ff}|$, in percent, shown only in grid cells where β_{nuc} was less than -0.25 ppm.

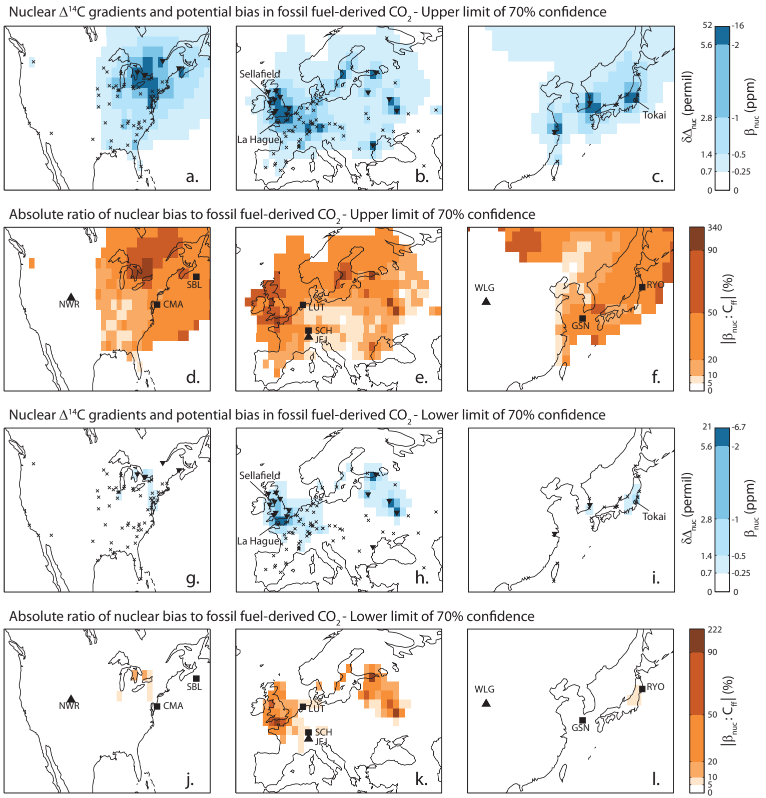

Fig. 3. Results from transport model simulations of ^{14}C emissions for 2005 estimated using emission factors at the upper and lower limits of the 70 % confidence intervals as shown in Fig. 1. Nuclear Δ^{14}C enhancement ($\delta\Delta_{\mathrm{nuc}}$) and potential nuclear bias to fossil fuel-derived CO_2 (β_{nuc}) for emissions at the upper **(a–c)** and lower **(g–i)** limits of 70 % confidence. The ratio $|\beta_{\mathrm{nuc}} : \delta C_{\mathrm{ff}}|$, in percent, shown only in grid cells where β_{nuc} was less than −0.25 ppm for emissions at the upper **(d–f)** and lower **(j–l)** limits of 70 % confidence.

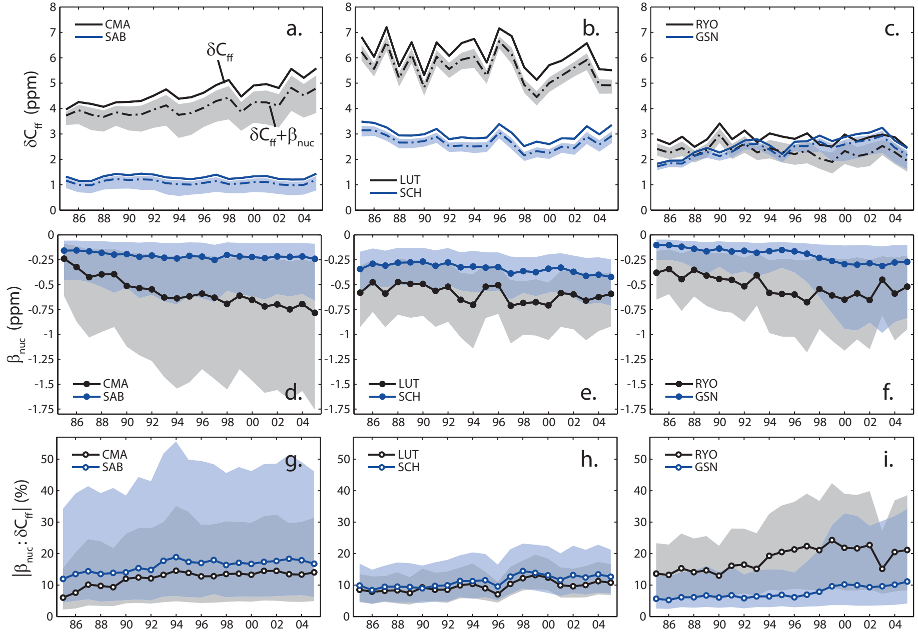

Fig. 4. (a–c) Annual mean fossil fuel-derived CO$_2$ (δC_{ff}, solid lines) and fossil fuel-derived CO$_2$ including the nuclear bias ($\delta C_{\text{ff}} + \beta_{\text{nuc}}$, dashed lines) simulated at each observation site for 1985–2005. **(d–f)** Annual mean β_{nuc} simulated at each observation site for 1985–2005. Panels **(g–i)** Annual mean ratio $|\beta_{\text{nuc}} : \delta C_{\text{ff}}|$ simulated at each observation site for 1985–2005, in percent. Filled areas show 70 % confidence intervals.

Title Page
Abstract | Introduction
Conclusions | References
Tables | Figures
◀| |▶
◀ ▶
Back | Close
Full Screen / Esc
Printer-friendly Version
Interactive Discussion